Variability of Basin-Scale Terrestrial Water Storage from a PER Water Budget Method: The Amazon and the Mississippi

NING ZENG

Department of Atmospheric and Oceanic Science, and Earth System Science Interdisciplinary Center, University of Maryland, College Park, College Park, Maryland

JIN-HO YOON

Department of Atmospheric and Oceanic Science, University of Maryland, College Park, College Park, Maryland

ANNARITA MARIOTTI

Earth System Science Interdisciplinary Center, University of Maryland, College Park, College Park, Maryland, and ENEA Climate section, Rome, Italy

SEAN SWENSON

University of Colorado, Boulder, Colorado

(Manuscript received 15 August 2006, in final form 17 April 2007)

ABSTRACT

In an approach termed the PER method, where the key input variables are observed precipitation P and runoff R and estimated evaporation, the authors apply the basin water budget equation to diagnose the long-term variability of the total terrestrial water storage (TWS). Unlike the typical offline land surface model estimate where only atmospheric variables are used as input, the direct use of observed runoff in the PER method imposes an important constraint on the diagnosed TWS. Although there is a lack of basin-scale observations of evaporation, the tendency of E to have significantly less variability than the difference between precipitation and runoff $(P - R)$ minimizes the uncertainties originating from estimated evaporation. Compared to the more traditional method using atmospheric moisture convergence (MC) minus R (MCR method), the use of observed precipitation in the PER method is expected to lead to general improvement, especially in regions where atmospheric radiosonde data are too sparse to constrain the atmospheric model analyzed MC, such as in the remote tropics.

TWS was diagnosed using the PER method for the Amazon (1970–2006) and the Mississippi basin (1928–2006) and compared with the MCR method, land surface model and reanalyses, and NASA's Gravity Recovery and Climate Experiment (GRACE) satellite gravity data. The seasonal cycle of diagnosed TWS over the Amazon is about 300 mm. The interannual TWS variability in these two basins is 100–200 mm, but multidecadal changes can be as large as 600–800 mm. Major droughts, such as the Dust Bowl period, had large impacts, with water storage depleted by 500 mm over a decade. Within the short period 2003–06 when GRACE data were available, PER and GRACE show good agreement both for seasonal cycle and interannual variability, providing potential to cross validate each other. In contrast, land surface model results are significantly smaller than PER and GRACE, especially toward longer time scales. While the authors currently lack independent means to verify these long-term changes, simple error analysis using three precipitation datasets and three evaporation estimates suggest that the multidecadal amplitude can be uncertain up to a factor of 2, while the agreement is high on interannual time scales. The large TWS variability implies the remarkable capacity of land surface in storing and taking up water that may be underrepresented in models. The results also suggest the existence of water storage memories on multiyear time scales, significantly longer than typically assumed seasonal time scales associated with surface soil moisture.

Corresponding author address: Ning Zeng, Department of Atmospheric and Oceanic Science, University of Maryland, College Park, College Park, MD 20742-2425.
E-mail: zeng@atmos.umd.edu

1. Introduction

Freshwater stored on the continents in the soil, at the surface, or underground is fundamental for life on land. These water reservoirs are also important for climate as they provide potential feedback mechanisms for climate variability (e.g., Yeh et al. 1984; Delworth and Manabe 1993; Zeng et al. 1999; Koster et al. 2004). Motivated in part by the prospect of improving seasonal-interannual climate prediction using the knowledge of soil moisture state, there has been significant interest in soil moisture variability in recent years.

Several methods have been used in obtaining soil moisture information, including in situ observations, satellite remote sensing, offline land surface model simulations, land data assimilation, and basin-scale budget analysis. Table 1 lists some of these methods and examples as well as their main characteristics. While being ground truth, in situ observations are limited in spatial and temporal coverage, mostly in a few regions, including the United States, former Soviet Union, and China. Models resolve soil moisture at high spatiotemporal resolution but are less constrained by observation. Satellite gravity measurements only have reliable information on scales larger than a few 100 000 km^2, that is, the size of a medium-size river basin. The two basin budget methods only give basin-scale soil water storage, but there is no fundamental limit on the basin size.

Each of these methods has its own advantages and limitations. There is limited understanding of the consistency or agreement of these often independent methods. While there is a reasonable understanding of the climatological seasonal cycles of all aspects of the hydrological cycle, there is a significant lack of knowledge on the interannual variability of terrestrial hydrological variables, including soil moisture.

While most other methods in Table 1 estimate near-surface soil moisture, the two basin budget approaches and the satellite gravity sensor measure total terrestrial water storage (TWS). This water storage includes moisture near the surface but also at the surface (snow and reservoir), deeper soil moisture, and groundwater (Fig. 1). Deep soil and groundwater variability may be particularly large (Rodell and Famiglietti 2001; Seneviratne et al. 2004). There is some confusion of terminology in literature as "soil moisture" is sometimes used to describe all the water on land. Here we make a clear distinction between the various components of the water storage versus the total (TWS) as shown in Fig. 1. For instance, a traditional land surface model simulates only soil moisture 1–2 m below the surface, which

would be smaller than the total water storage discussed in this paper.

Much emphasis has been on near-surface soil moisture, partly because seasonal crops in agriculture are typically shallow rooted. However, trees, shrubs, and some natural grasses can have very deep roots that have been observed to take water from deep soil and groundwater, for instance, below 8 m over the Amazon (Nepstad et al. 1994), 5–20 m in Edwards Plateau, Texas (Jackson et al. 1999), and 7 m in Arizona (Davis and Pase 1977). Recent research has suggested the potential importance on land hydrology and climate of such variability through plant deep root water uptake (Kleidon and Heimann 2000; Jackson et al. 2000; Amenu et al. 2005). In addition to the apparent effects of irrigation and drinking water usage, the role of underground water in climate may also be more important than once thought. The ability of forest roots to use deep water in the Amazon is critical in sustaining the large dry season evapotranspiration (Shuttleworth 1988; Nepstad et al. 1994) and further influencing climate through water vapor recycling. When deeper water storage is utilized by vegetation, the dynamic range of effective field capacity becomes larger and leads to a longer land water memory that may be of importance to climate variability. There is, thus, a strong need in knowing how water storage, especially in the lower part, varies over time and space.

In general, observations have been too short to demonstrate decadal soil moisture variability, but such information is becoming available for a few places, such as the Ukraine (Robock et al. 2005) and Illinois (Hollinger and Isard 1994; Yeh et al. 1998; Rodell and Famiglietti 2001). Here we propose a new application of the basin-scale water budget equation termed PER method, where the key input variables are observed precipitation P and runoff R and evaporation E. In addition to seasonal-interannual variability, the PER method presented here can provide useful information on decadal and longer timescale water storage variability, limited mainly by the length of precipitation and runoff data. This method is to apply the simple basin water budget equation to diagnose the long-term variability of TWS using observed precipitation and runoff and estimated evaporation. We present the method in section 2 and contrast it with the more traditional method using atmospheric moisture convergence and runoff, also with typical offline land surface modeling. We then discuss the seasonal cycle and interannual variability from this method for the Amazon basin in sections 3 and 4, and compare the results with the moisture convergence method and satellite gravity-based observations. In section 5, the long-term TWS variabil-

TABLE 1. Methods commonly used to estimate soil moisture variability.

Method	Examples	Advantages	Limitations	Degree of observational constraint
In situ	Global soil moisture data bank[a]	Direct measurement	Point data; limited coverage; near surface	High
Remote sensing microwave	Microwave[b]	High spatial and temporal resolution	Surface; area sparsely vegetated	High
Remote sensing gravity	GRACE[c]	Independent; total column	Low resolution; only since 2002	High
Offline land model forced by atmospheric variables	GSWP[d]; PDSI[e]	High spatial and temporal resolution	Model dependent; top soil layers	Medium
Data assimilation model + observation	GLDAS[f]	High spatial and temporal resolution	Model dependent; top soil layers	Medium-high
Basin-scale budget MCR	Rasmusson (1968)	Long-term; total column	Basin only; sensitive to quality of atmospheric data	Medium
Basin-scale budget PER	This study	Long-term; total column	Basin only; some uncertainty in evaporation	Medium-high

[a] Robock et al. (2000).
[b] Engman and Chauhan (1995).
[c] Tapley et al. (2004) and Wahr et al. (2004).
[d] Dirmeyer et al. (1999).
[e] Palmer drought severity index.
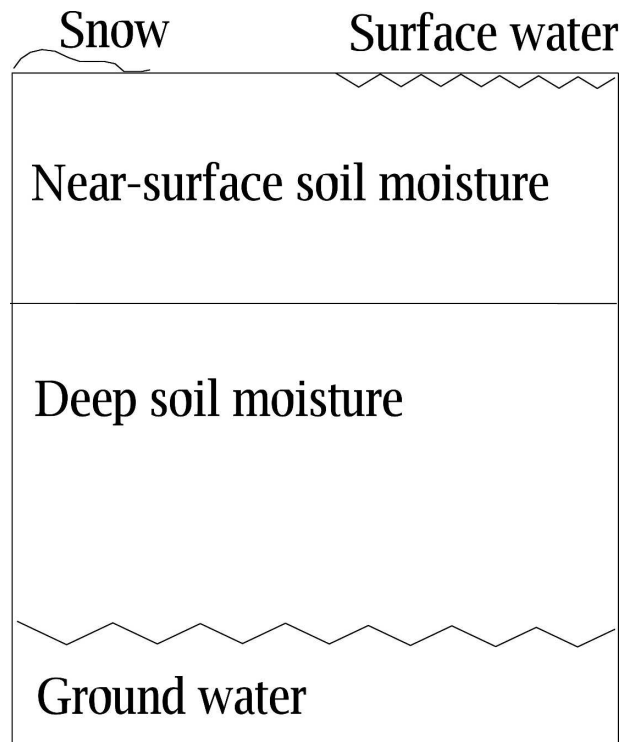[f] Global Land Data Assimilation System: Rodell et al. (2004a).

FIG. 1. Major components of total land water storage. Traditional methods, including in situ soil moisture measurements and land surface modeling, have focused on the near-surface component. This study focuses on the TWS using basin budget PER method.

ity is presented for the Mississippi basin. Uncertainties of the method are discussed in section 6, followed by a comparison with the newly available Gravity Recovery and Climate Experiment (GRACE) satellite data for 2003–06 (section 7) and conclusions in section 8.

2. Methodology, data, and models

a. Basin budget method for total water storage: MCR

The traditional moisture convergence method (termed MCR here; Rasmusson 1968; Roads et al. 1994; Masuda et al. 2001; Zeng 1999; Seneviratne et al. 2004) considers the atmosphere and land surface over a drainage basin as one single box, thus precipitation and evaporation vanish as interior fluxes for the total water budget. In this method (Fig. 2), moisture convergence (C; the vertically integrated water vapor flux) and observed streamflow for the drainage basin (runoff integrated over the whole basin) are integrated to obtain the change in atmosphere W and soil water storage S:

$$\frac{d(W + S)}{dt} = C - R. \qquad (1)$$

Using the recent atmospheric reanalyses, this method appears to produce reasonable estimates of the seasonal cycles and in some cases year-to-year variability over several basins around the world [Roads et al.
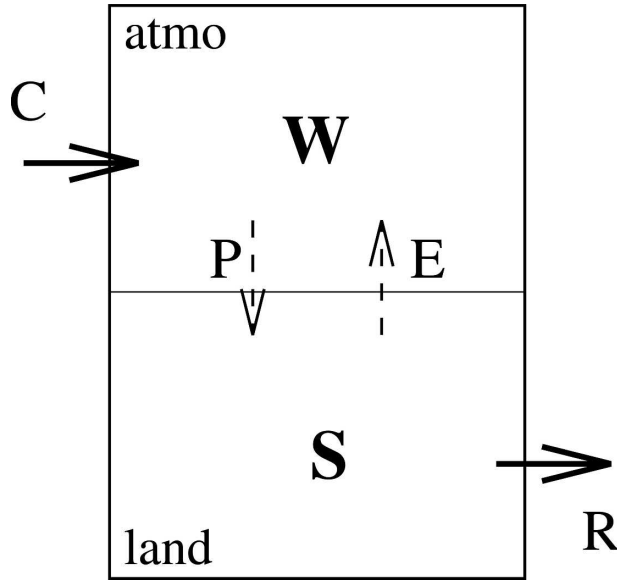
FIG. 2. The moisture convergence method in diagnosing basin-scale soil moisture variability. The atmosphere and land are treated as one single box such that the total water storage ($W + S$) can be diagnosed as a time integral of moisture convergence (C; from atmospheric analysis) $-$ R (observed); P and E are not needed because they are interior fluxes. Adapted from Zeng (1999).

(1994); Zeng (1999); Seneviratne et al. (2004); change in W is typically much smaller than that of S]. However, on decadal and longer time scales, the results are less robust especially over remote tropical regions, such as the Amazon. Our analysis (not shown) suggests that the lack of radiosonde data in these regions left the host atmospheric model poorly constrained and the simulation of convective rainfall is one of the weaker aspects of the models. Artificial jumps in the reanalysis systems when different observations are injected (Kalnay et al. 1996; Betts et al. 2005) may also be important. Such problems may be significantly alleviated if the observed precipitation is used in place of moisture convergence because precipitation is generally a better observed quantity over a longer period of time, and this leads to the PER method.

b. Basin budget method for total water storage: PER

In the PER method, only the land surface is considered (Fig. 3). The water budget equation for the land box is

$$\frac{dS}{dt} = P - E - R, \qquad (2)$$

where S is the total terrestrial water storage, P is precipitation, and E is evaporation (for simplicity, we use
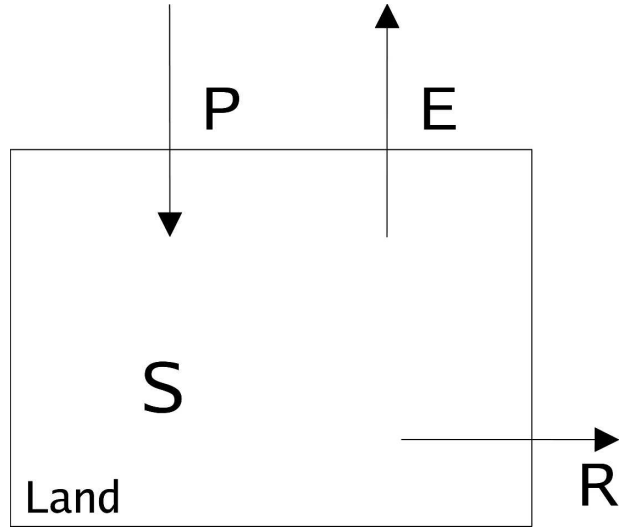

FIG. 3. Vertically integrated land water budget. Total S is a time integral of $P - E - R$. In the PER method, P and R are from observations while E needs to be estimated using model. In contrast, a typical offline land surface model uses only observed P while E and R are modeled.

evaporation and evapotranspiration interchangeably here).

In this method, precipitation and runoff are observed, and evaporation may be estimated using a land surface model driven by observed precipitation and other atmospheric variables (see caveats below in section 2c). Thus the water budget Eq. (2) can be explicitly written for this method as

$$\frac{dS}{dt} = P_{\text{obs}} - E_{\text{est}} - R_{\text{obs}}, \qquad (3)$$

where the subscript "obs" denotes "observation," and "est" denotes "estimate." Compared to the moisture convergence method, the PER method uses observed P and R, thus more observational constraint. In contrast, offline land surface model uses only observed P as input (section 2e).

Similar to the moisture convergence method (Rasmusson 1968; see discussions of this technique in Zeng 1999), a constant correction is added to E such that $P - E^* - R$ ($E^* = E +$ correction) integrated over the analysis period is zero. As a result, the diagnosed TWS has the same value at the beginning and the end of the integration. This is equivalent to removing a linear trend in TWS. This correction is necessary as typical estimation of E tends to have systematic bias when compared to $P - R$, as indicated by the vertical shifts of E estimates relative to $P - R$ in Fig. 4. This bias can easily result in unrealistically large drift (trend) in the integrated S [e.g., Fig. 6c of Zeng (1999) and Fig. 9a of
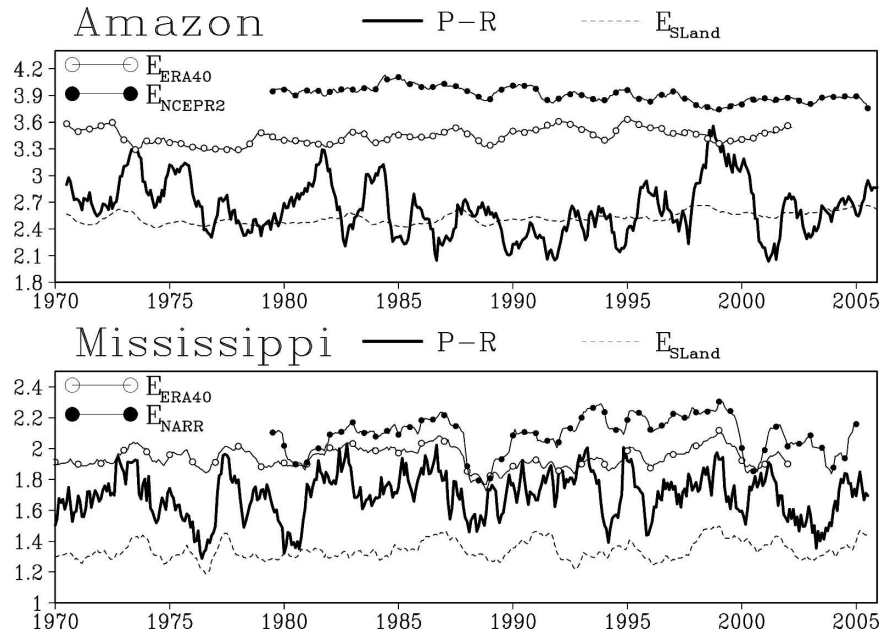
FIG. 4. Here E estimated from the SLand model and ERA-40, NCEP R2, and NARR reanalyses compared to observed $P - E$ (mm day^{-1}). The uncertainty in diagnosed water storage [Eq. (3)] due to the estimated E would be small if E variability is significantly smaller than that of $P - E$. Seasonal cycle has been removed using a 12-month running mean.

Seneviratne et al. (2004) for similar situations in MCR method]. For instance, because E in the National Centers for Environmental Prediction–Department of Energy (NCEP–DOE) reanalysis-2 (NCEP R2; Kanamitsu et al. 2002) is about 1 mm day^{-1} larger than $P - R$ (Fig. 4a), the imbalance without E correction would lead to about a 365-mm drift at the end of the first year, so that the diagnosed S would go out of range in 2–3 yr (e.g., Fig. 6b). Although simple-land (SLand; Zeng et al. 2000; see description below in section 2e) has a rather small bias in the Amazon, it is larger in the Mississippi. Thus this is a fundamental limitation of this method in that only the relative changes within the integration period can be inferred from such methods. But the relative variations within the period still provide valuable information not readily available otherwise.

c. Potential weakness of the PER method: Evaporation

The main potential weakness of the PER method is that basin-scale evaporation is generally not available and needs to be estimated. Should such estimates introduce large error, uncertainty would be large in the diagnosed water storage. Equation (3) indicates that a sufficient criterion is for the variation of E_{est} to be significantly smaller than that of $P_{obs} - R_{obs}$. Because the

magnitude of variation is often time scale dependent, this criterion may differ, for instance, on seasonal versus interannual time scales.

Observational evidence suggests that evaporation indeed tends to have relatively small variation. Field measurements at the heart of the Amazon rain forest show a rather small seasonal amplitude in evaporation despite the large seasonal cycle in precipitation and soil moisture (Shuttleworth 1988; Werth and Avissar 2004). In the extratropics, such as the Mississippi basin where radiation (thus potential evaporation) has large seasonal cycle, the seasonal amplitude of E can be large, but the interannual variation is much smaller. To assess the uncertainty introduced by estimated evaporation, we have analyzed the evaporation from the model SLand (Zeng et al. 2000) and from the following reanalysis products: the 40-yr European Centre for Medium-Range Weather Forecasts (ECMWF) Re-Analysis (ERA-40; Gibson et al. 1997), NCEP R2 (Kanamitsu et al. 2002), and the North American Regional Reanalysis (NARR; Mesinger et al. 2006). The reanalysis E was also simulated by the embedded land surface model, which is typically more sophisticated than SLand. The results (Fig. 4) show that the variance of interannual variability in E is smaller than $P_{obs} - R_{obs}$ by a factor of 3 to 8 (as measured by standard deviation) over the Amazon, while for the Mississippi it

is a factor of 2 to 3 smaller. This of course does not exclude possible larger uncertainties for particular events. For instance, the changes in NARR evaporation in 1988 and 1999 are comparable to $P - R$, with consequences that will be discussed in section 6. Thus, in the worst-case scenario, even if the estimated E_{est} is completely out of phase with the (unknown) truth, the diagnosed water storage would still reflect the dominant signal from $P_{obs} - R_{obs}$. In practice, the uncertainty would be smaller than the worst-case scenario because the model estimate can capture the variability in E to some degree because it is mainly driven by observed precipitation and radiation. The resulting uncertainties in diagnosed TWS will be assessed in section 6 using multiple evaporation estimates.

d. Forcing data for the PER and MCR method

To study the TWS variability in the Amazon and Mississippi drainage basin using the PER method, the observed gauge-based precipitation for 1901–2002 from the Climate Research Unit of the University of East Anglia (CRU; New et al. 1999; Mitchell and Jones 2005) was used in Eq. (3). Precipitation from the gauge-based Precipitation Reconstruction over Land (PRECL; Chen et al. 2002) dataset for 2003–06 was merged with CRU to produce a "control" precipitation dataset that was used for most of the analysis unless otherwise specified. We also used precipitation from the satellite–gauge blended Climate Prediction Center (CPC) Merged Analysis of Precipitation (CMAP; Xie and Arkin 1996) dataset, and the uncertainties due to the use of these three different precipitation datasets will be discussed in section 6.

The monthly historical streamflow records for the Amazon River at Obidos and for the Xingu River at Altamira were used to reconstruct the Amazon basin runoff, following the method used by Zeng (1999). The Amazon runoff data are from the Brazilian National Water Agency (ANA). The data are noninterrupted from 1970 to 2006. The historical streamflow of the Mississippi River basin observed at Vicksburg, Mississippi, extends only to September 1998 [obtained from the National Water Information System, U.S. Geological Survey (USGS) Web site http://waterdata.usgs.gov/nwis/]. Recent record of the streamflow is estimated based on the daily data of water height observed at the same location [0800 central standard time (CST) reading], which is obtained from http://rivergages.com maintained by the U.S. Army Corps of Engineers. Following Qian et al. (2007), a simple linear regression between the streamflow and the river height for the period of 1948 till 1997 provided the long-term streamflow data (S = river level $\times$ 0.07452 + 0.06102). The

long-term variability from 1928 to 2006 for the Mississippi basin will be analyzed.

Evaporation is estimated using an offline simulation of SLand (section 2e) forced by the CRU precipitation (but PRECL or CMAP is used for sensitivity experiments discussed in section 6). Here, E^* estimated using SLand will be the "control-case" evaporation and will be used in all of the analysis and figures unless otherwise specified. For comparison, we will also show results using the ERA-40, NCEP R2, and NARR reanalysis evaporation products as discussed in section 2c above. The precipitation and evaporation data were aggregated to the drainage basin of interest as basin averages, and Eq. (3) was integrated at monthly time step to obtain S, with an arbitrary integration constant. Section 6 will also discuss the uncertainty due to the use of different evaporation estimates from SLand, ERA-40, NCEP R2, and NARR.

For the MCR method for the Amazon seasonal cycle in section 3, moisture convergence from the reanalyses NCEP–National Center for Atmospheric Research (NCAR; Kalnay et al. 1996), ERA-40 (Gibson et al. 1997), and Goddard Earth Observing System version 1 (GEOS1; Schubert et al. 1993) is used in addition to the runoff above.

The Southern Oscillation index (SOI) is used as an index for the atmospheric variability over the tropical Pacific Ocean for comparison purpose because the Amazon climate and hydrological variability are significantly influenced by the El Niño–Southern Oscillation (ENSO; e.g., Zeng 1999).

e. Land surface model and the GRACE gravity data

In a one-layer land surface model running in offline mode (i.e., not interacting with the atmosphere), Eq. (2) is forced by P, while E and R are simulated (parameterized) as functions of S [and also precipitation, radiation, and other variables and parameters (see, e.g., the bucket model of Manabe et al. 1965 or the SLand model of Zeng et al. 2000)]:

$$\frac{dS}{dt} = P_{obs} - E_{mod}(S) - R_{mod}(S), \qquad (4)$$

where the subscript "mod" denotes "modeled."

The precipitation from the CRU dataset and surface air temperature from the National Aeronautics and Space Administration (NASA) Goddard Institute for Space Studies (GISS; Hansen et al. 1999) were used in conjunction with the climatological values of surface wind and vapor pressure, along with radiation from the NCEP–NCAR reanalysis to drive an offline model
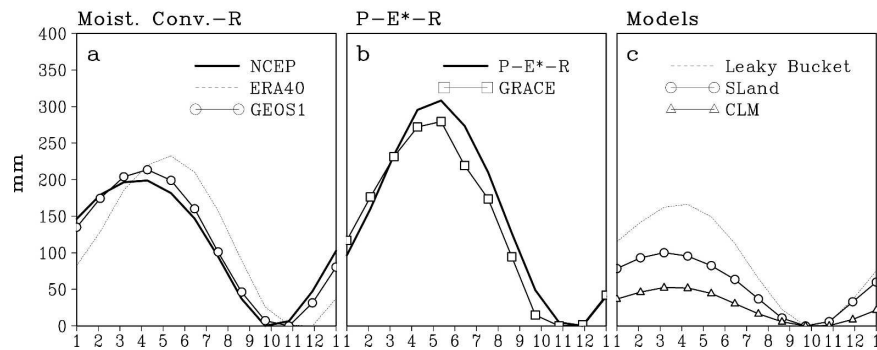
Amazon Seasonal Cycle

FIG. 5. Seasonal cycle of Amazon S using (a) the MCR method with moisture convergence from three reanalyses; (b) the PER method using observed P, R, and SLand model estimated E and that derived using GRACE satellite observations (Fig. 11); (c) simulated by three offline land surface models (SLand, CPC leaky bucket, and CLM) forced by observed atmospheric variables.

SLand (Zeng et al. 2000) coupled to a dynamic vegetation model Vegetation–Global–Atmosphere–Soil (VEGAS; Zeng et al. 2005). The model was run at $1° \times 1°$ resolution at daily time step and the results were then aggregated over the studied basin for the budget analysis at monthly time steps.

The CPC leaky bucket model was run similarly as SLand, driven by precipitation from PRECL and air temperature from NCEP–NCAR reanalysis 1 (Fan and van den Dool 2004). Compared to SLand, which has a field capacity of 500 mm, the leaky bucket model has a 750-mm field capacity.

In a multilayer land surface model, a similar budget equation can be obtained if all the layers are vertically integrated. It is beyond the scope of this paper to describe them, and the readers are referred to Shao and Henderson-Sellers (1996) for a summary of such models. Here we will use one such model, the Common Land Model (CLM; Dai et al. 2003). Used here is soil moisture integrated from the surface to 3 m below from the Community Land Model, version 3 (CLM3) that was forced by PRECL and the Global Precipitation Climatology Project (GPCP) merged precipitation (Qian et al. 2007). While SLand, the leaky bucket, and CLM results are used here for comparison with the PER method, the extent is limited as the focus here is to demonstrate the feasibility of a new technique, rather than a comprehensive intercomparison study.

The advent of recent satellite gravity-based measurement from NASA's GRACE mission provides an independent means to validate the interannual variability of the diagnostic method (Tapley et al. 2004; Wahr et al. 2004). The variation in the earth's gravity field as measured by multiple satellites from space indicates largely the changes in water mass distribution. The resolution

of such technique is inherently low compared to other methods, but it depicts broad-scale changes in the hydrological cycle not easily obtainable using other methods. Because there is no relevant data to compare, GRACE error is estimated by comparison with data-constrained numerical models (Wahr et al. 2004). At the current stage, error in the measured equivalent water thickness (equivalent to TWS as defined here) is 15 mm with 1000-km smoothing (Gaussian half-width). The error increases at higher resolution, and it is 30% better with 1500 km smooth, while 40% worse for 750 km smoothing. In this paper, we somewhat arbitrarily chose 500-km resolution to strike a balance between resolving the two studied basins and reducing GRACE's intrinsic error. The results are shown in sections 3 (Amazon seasonal cycle) and 7 (interannual variability for the Amazon and Mississippi).

3. Seasonal cycle over the Amazon basin

After applying the PER method to the Amazon basin following Eq. (3), using the data input described in section 2, a monthly time series of S was obtained. A climatological seasonal cycle was then derived as the average of the 37-yr (1970–2006) diagnosed total land water storage. Figure 5 shows the seasonal cycle for the Amazon basin. The three MC method analyses (Fig. 5a) have similar seasonal amplitude of 175–200 mm, while the satellite gravity-based estimate from GRACE and the PER method have an amplitude of about 300 mm (Fig. 5b). The three offline land models, SLand (Zeng et al. 2000), the leaky bucket model (Fan and van den Dool 2004), and CLM (Dai et al. 2003), have an amplitude ranging from 50 to 150 mm. Both GRACE and the PER method give a maximum in April–May and a minimum in October–November after the drier
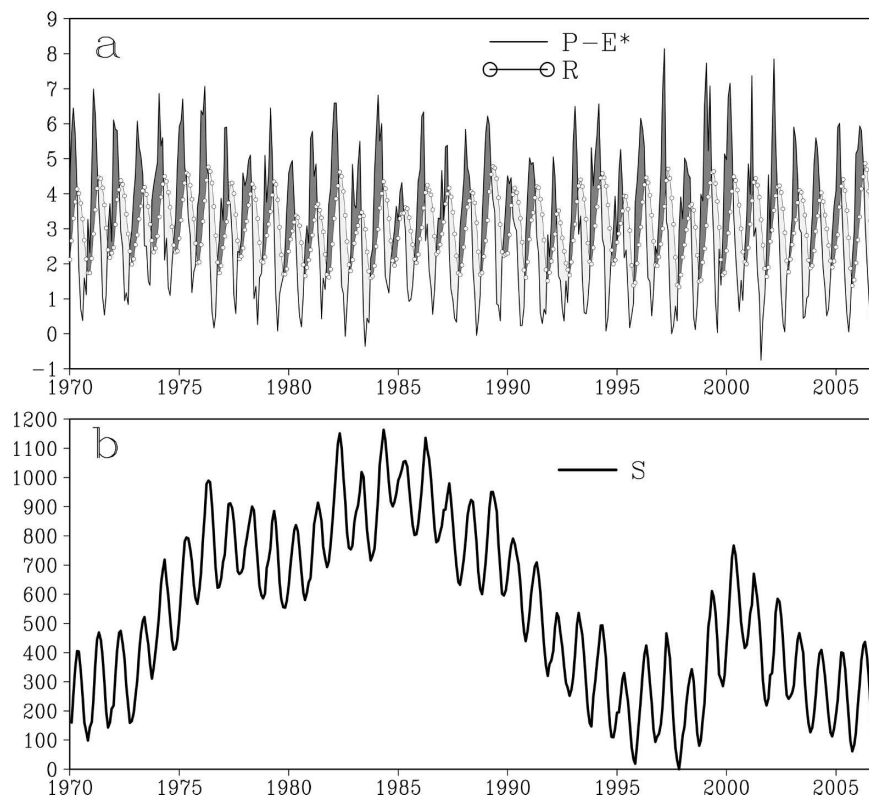
Amazon : PER method

FIG. 6. (a) Variabilities of $P - E^*$ and R in mm day^{-1}; (b) the diagnosed Amazon soil moisture in mm. When $P - E^*$ is greater than R, the soil water storage increases, undergoing a recharge period (heavy shading); when $P - E^*$ is less than R, the soil undergoes a discharge (light shading). There is a strong seasonal cycle but also with comparable or larger interannual–interdecadal variabilities.

boreal summer (the basin averages tend to be dominated by the larger southern Amazon). The models and reanalyses produced maximum and minimum somewhat earlier by 1–2 months.

To the extent that GRACE measurement can be considered as a good observation of the basin-scale water storage, the PER method appears to capture this observed change. The reanalyses and the offline models thus tend to underestimate somewhat the seasonal cycle amplitude in the Amazon. Given the uncertainties in all these methods and large interannual variability (below), the seasonal cycle of Amazon water storage can be given as 250 ± 100 mm. However, the two basin budget methods (GRACE and $P - E$) include all the changes from surface to underground water, thus providing an upper limit to the models, which normally include only a fraction of the active soil moisture as discussed further below. A caveat we emphasize is that such a conclusion can differ for different basins as data

quality and model may behave very differently at different places.

4. Amazon interannual and decadal variability 1970–97

Figure 6a shows the water input ($P - E^*$) and the observed runoff R of the Amazon basin at monthly resolution. There is a robust seasonal cycle over which $P - E$ surpasses R during winter and spring, when land water storage is recharged. The input $P - E$ is less than R from early summer to fall when TWS is discharged (Fig. 6b; the term "discharge" is used here to indicate the "recharge–discharge" of soil water holding capacity, not to be confused with "river discharge" to which we refer to as streamflow or runoff). Overall, R has a seasona amplitude about a factor of 2 smaller and a phase lag of 3–4 months relative to $P - E^*$ (also see Zeng 1999). This reduced amplitude and phase lag is
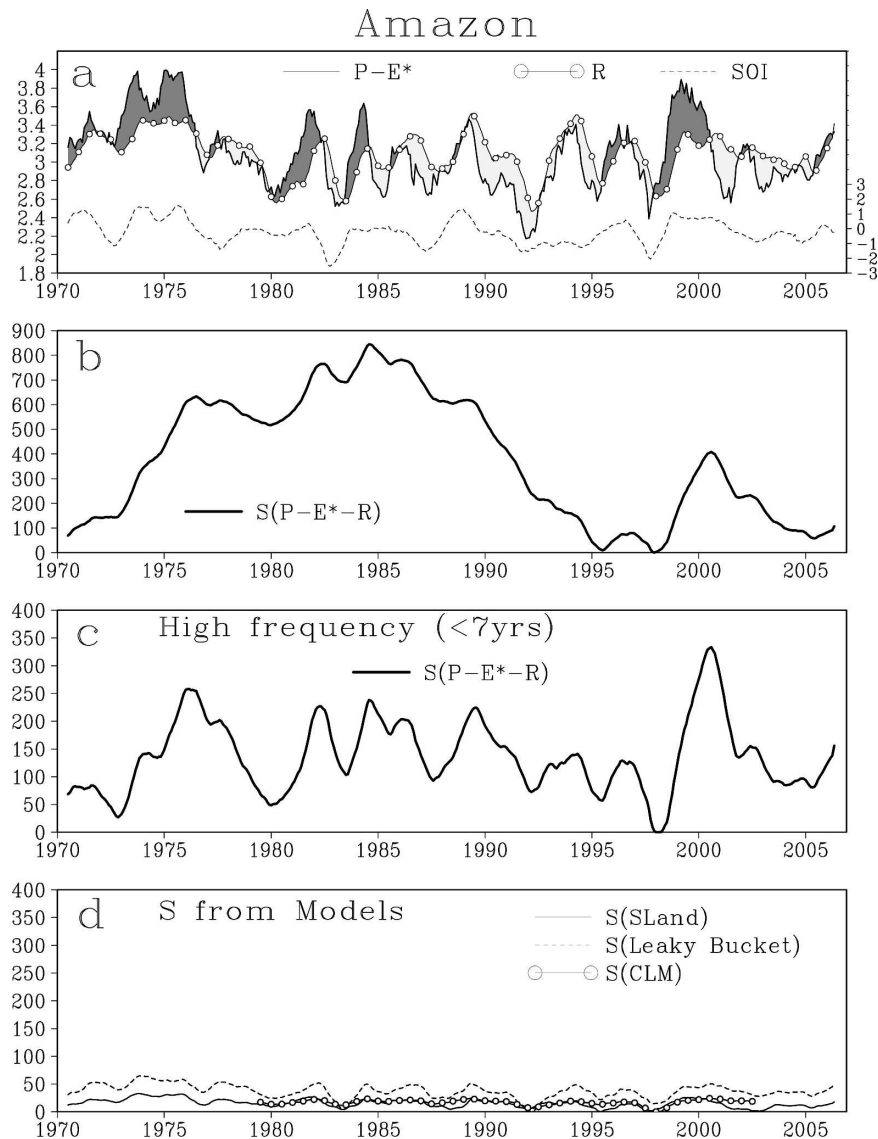
Amazon

FIG. 7. (a) Variabilities of $P - E^*$ and R in mm day^{-1} and the SOI (labeled on the right in mb); (b) the diagnosed Amazon S (mm) from the PER method; (c) same as in (b) except for the high frequency component (higher than 7 yr, i.e., interannual but not decadal and longer); (d) S simulated by 3 models: SLand, Leaky Bucket, and CLM. A major recharge period occurred during two large La Niña events in 1974–75, and a major discharge period was associated with the protracted El Niño of 1991–93. Note the small amplitude in S from models compared to the PER method. Seasonal cycle was removed by a 12-month running mean.

typical because TWS is a damped and delayed response to the driving precipitation due to its memory effect.

The diagnosed TWS shows large interannual to interdecadal variability on which the seasonal cycle is superimposed. The long-term variability can be seen more clearly by filtering out the seasonal cycle using a simple 12-month running mean (Fig. 7b, solid line). On multidecadal time scales, there is a major recharge period from 1971 to 1985, followed by a discharge afterward (Figs. 7a,b). The minimum to maximum differ-

ence over the 37 yr is about 800 mm. We note again that, the correction in E^* (section 2b) removes any long-term trend so that over the whole analysis period there is no net gain in soil water storage. Thus the lowest frequency change can only be viewed as relative, that is, the general decrease since 1985 is only relative to the increase in the previous 15 yr.

The large change of up to 800 mm in TWS is remarkable, as many current land surface models have field capacity (the maximum change in soil moisture a model

can produce) comparable to this, and the earlier bucket model had a field capacity of only 150 mm (Manabe et al. 1965). Although we currently have no other means to validate the magnitude of such long-term change, the general variation (ups and downs) can be assessed because Amazon hydrological cycle is dominated by ENSO-related interannual variability. For instance, the period with largest recharge during 1974–75 corresponds to two major La Niña events before the 1976–77 decadal climate shift in the Pacific Ocean, as indicated by the SOI. In the other direction, the major discharge period of the early 1990s was caused by the protracted El Niño of 1991/93 and that of 1986/87.

A simple high-pass filter was applied to the diagnosed TWS in Fig. 7b to remove the frequencies lower than 7 yr. The remaining signal is mostly interannual (Fig. 7c), showing decreasing TWS during events, such as the 1982/83 El Niño. However, even in this case, the major peaks reflect the lower frequency variations, such as the two La Niña events around 1975 and the early 1990 El Niño. Plotted in Fig. 7d are the model-simulated soil moisture from SLand and the CPC leaky bucket model, and both show significantly smaller variability at about 1/3 of the diagnosed TWS amplitude on interannual time scales, while the decadal and longer-term variability is even smaller (cf. Fig. 7b).

Such large differences especially on longer time scales are striking. While the PER method may overestimate the amplitude of these slow variations (section 6), the models appear to significantly underestimate it. One contributor of the smaller model changes is that current land surface models typically only represent the water holding capacity of the top 1–2 m of soil. Among the two one-layer models, SLand has a field capacity of 500 mm, while the leaky bucket model has a field capacity of 750 mm. Interestingly, the multilayer model CLM has a variability with amplitude comparable to SLand. Thus it is understandable that these models underestimate the multidecadal change that is comparable to the model field capacity. However, simple increase in model soil depth may not be sufficient if deep soil water cannot be utilized by vegetation. On the other hand, the phasing of the models agrees reasonably well with the PER result and among themselves (Figs. 7c,d). It remains to be seen how other complex land models and data assimilation systems compare with the water budget and satellite results.

5. Variability in the Mississippi basin from 1928 to 2006

Data quality and model may behave very differently from basin to basin, especially across different climatic regimes. It is thus of great interest to see how the PER method works for midlatitude regions. We have applied the method to the Mississippi basin (Fig. 8). The total water storage (Fig. 8b) in the Mississippi decreases by about 400 mm from the 1920s to the end of the 1930s (the Dust Bowl period), followed by a recharge period in the 1940s. The drought in the 1950s plunged soil moisture to the lowest level and then recovered to high level during the following two decades of pluvial period (Seager et al. 2005). Smaller drought events also left their impact on TWS, such as 1988. The long-term change from low in the 1930s and 1950s to the high in the late 1990s is about 600 mm. Further analysis (not shown) suggests that these changes are largely influenced by the west part of the basin, in particular, the Great Plains region. Since the western part of the Mississippi basin is semiarid, while the east side is temperate humid, and the climate varies greatly across the basin, the basin average analysis may mute some of the more interesting regional changes. For instance, during the recent 1998–2002 drought of the American West (Hoerling and Kumar 2003; Seager et al. 2005), the Mississippi total water storage dropped by about 120 mm, significantly smaller than the change in earlier decades.

On interannual time scales shorter than 7 yr (Fig. 8c), the amplitude of interannual variability is about 100 mm. Such an amplitude is comparable to the total water storage variability based on in situ observations of the major components of the TWS for Illinois (Rodell and Famiglietti 2001), if the assumption can be made that Illinois is representative of the whole Mississippi basin. Interestingly, the two-model simulated soil moisture has interannual amplitude much closer to the diagnosed one than in the Amazon case (Fig. 8d). In both cases, the phase relationships are generally in good agreement (not surprisingly because they all reflect the signal in the precipitation forcing). However, the decadal and interdecadal variabilities in the two models are still much smaller than the diagnosed.

One implication of the diagnosed variability in Fig. 8b is potentially very long memory in terrestrial water storage, including soil moisture. For instance, the discharge during the Dust Bowl period is somewhat larger than that of the 1950s drought, as seen by the larger shaded area with negative $P - E^* - R$ values for the 1930s in Fig. 8a, yet TWS is at a minimum at the end of the 1950s drought. This is because the recharge in the 1940s is not sufficient to recover the water loss in the 1930s. Thus in a way the memory of the Dust Bowl period was not forgotten until a few decades later. While uncertainties in the data and methodology may hamper the accuracy of such detailed interpretation,
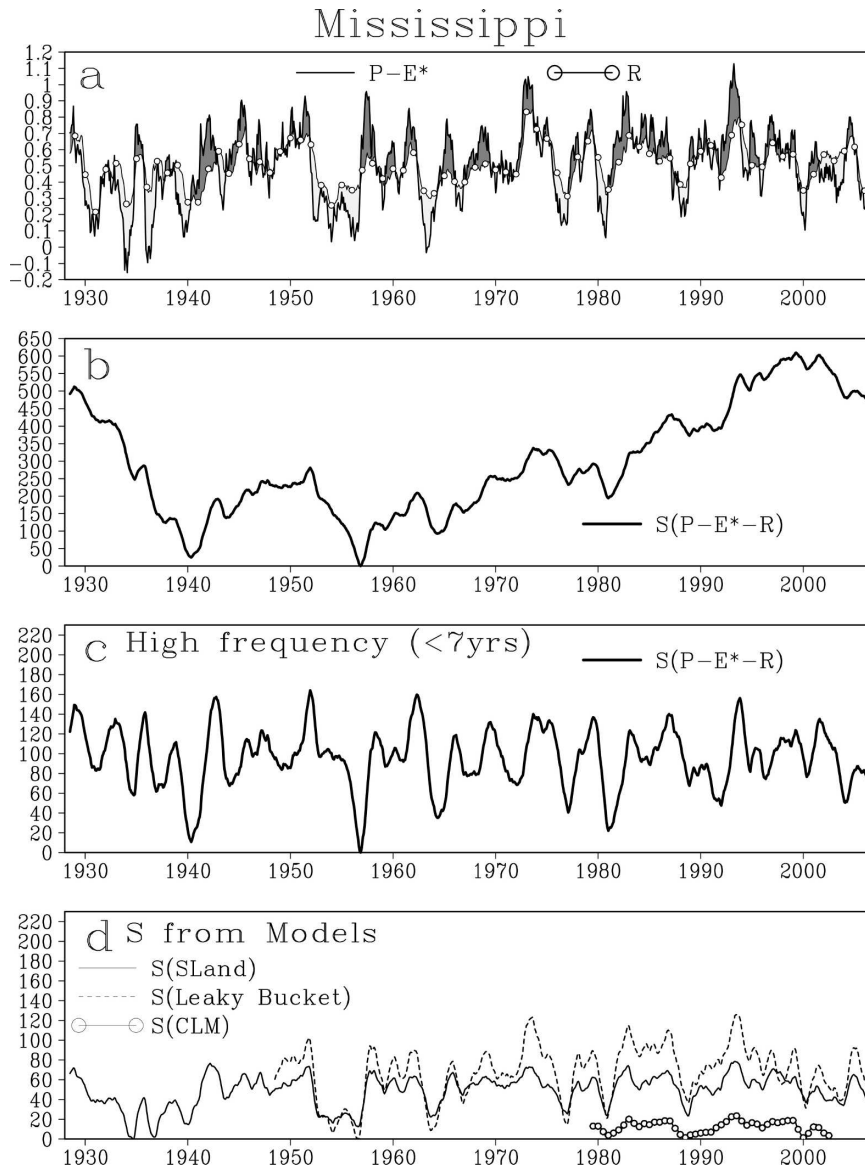
FIG. 8. Same as in Fig. 7 but for the Mississippi basin. The major discharge periods are the Dust Bowl in the 1930s and the drought in the 1950s. A major recharge took place during the pluvial period from the 1960s to the 1990s.

the results nonetheless suggest a significantly longer water storage memory than typically assumed.

6. Uncertainties due to errors in *P*, *E*, and *R*

To quantify impact on *S* due to the uncertainties in observed precipitation, we used three different precipitation datasets: CRU (our control case that has been used in previous sections), PRECL, and CMAP in Eq. (3) to diagnose *S*. Here, *E* was derived using SLand with the corresponding *P* as forcing (identical *E* was also used in sensitivity runs, and the results are very

similar). The PER method was applied to the period of January 1982–December 2002 so that the overall trend may be different from the longer data shown in Figs. 7b and 8b. The TWS derived using different precipitation datasets show general agreement for both the Amazon and Mississippi (Fig. 9), especially between the two gauge-based datasets CRU and PRECL, while the satellite–gauge blended CMAP results are somewhat more different. The correlation between *S* derived from the three precipitation datasets ranges from 0.45 to 0.79 (Table 2, upper row). The ratio of standard deviation ranges from 0.54 to 1.93, thus the amplitude uncertainty
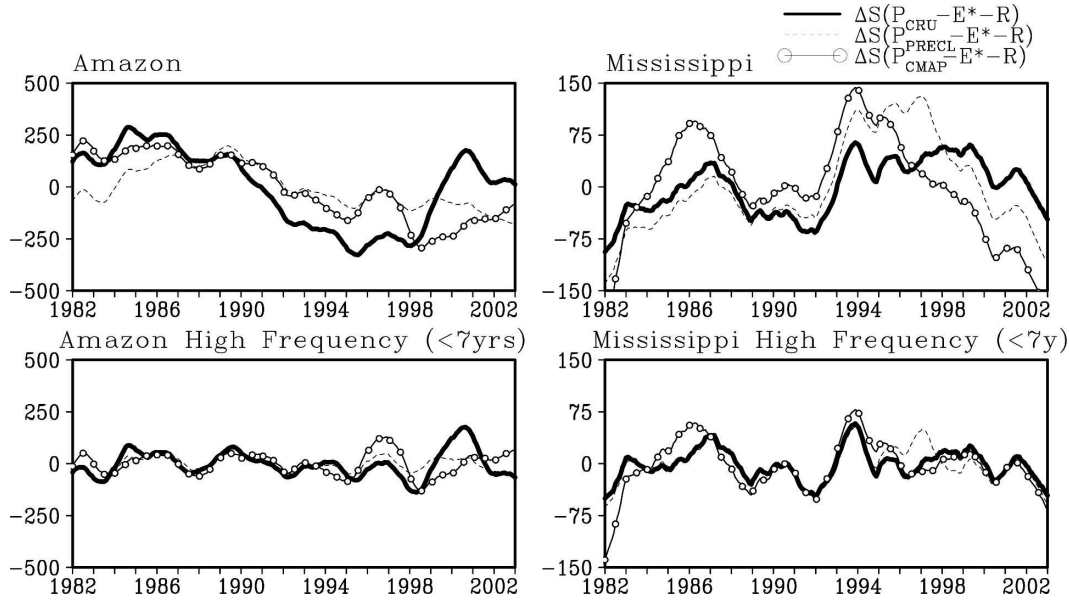
FIG. 9. Relative ΔS (mm) diagnosed by the PER method using three different precipitation datasets CRU, PRECL, and CMAP. Evaporation was estimated using the SLand model forced by the corresponding precipitation. Correlation and relative amplitude are listed in Table 2. These indicate the uncertainty in the PER method due to uncertainties in the observed precipitation forcing data.

can be close to a factor of 2. The high frequency component derived using a high-pass filter with cutoff at 7 yr shows significantly better consistency among the three datasets (lower two panels of Fig. 9), with correlation ranging from 0.33 to 0.83 and the σ ratio from 0.57 to 1.64 (Table 2, lower row). A quick inspection of Fig. 9 shows that nearly all the interannual variations are in agreement, and the amplitude mismatch occurs for few events.

We argued in section 2c that estimated evaporation may be a main potential source of uncertainty because precipitation and runoff are observed [Eq. (3)]. Figure 10 shows the results from using different evaporation estimates. The different evaporation estimates give generally similar S, especially on interannual time scales (less than 7 yr). The correlation is from 0.69 to 0.98 and the ratio of standard deviation is from 0.98 to 1.27, excluding NARR (Table 3). A major discrepancy

occurs between S from NARR and the other two, mostly in two periods around 1988 and 1999, such that the correlation is -0.12 (not significant at the 95% confidence level) with SLand. This discrepancy corresponds to the large changes in E from NARR for this period that are comparable to changes in $P - E$ (section 2c and Fig. 4). It is not clear why NARR evaporation can be so different from the other two, and such differences need to be better understood before we have confidence in the long-term S variability derived this way. An additional caveat is that all these evaporation estimates are model based, thus possibility remains that actual E may have larger variability than depicted by these estimates.

Another source of uncertainty may come from the fact that the observational systems of precipitation and runoff may have changed over time, for instance, due to the replacement of instrumentation or changes in mea-

TABLE 2. Uncertainty in the PER method due to different precipitation datasets. "Corr" is the correlation between S from PRECL or CMAP and CRU; "σ/σ" is the ratio of the corresponding standard deviations; "Total" is the full time series of S, while "HF" is its high frequency component with a period less than 7 yr.

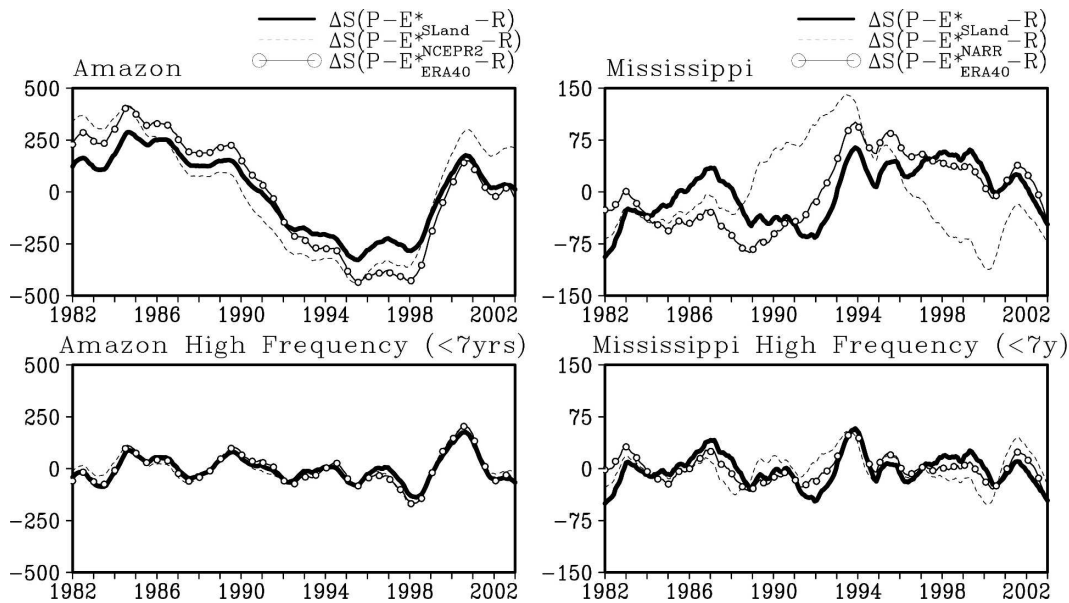|	Amazon				Mississippi			
	PRECL/CRU		CMAP/CRU		PRECL/CRU		CMAP/CRU	
	Corr	σ/σ	Corr	σ/σ	Corr	σ/σ	Corr	σ/σ
Total	0.51	0.54	0.63	0.83	0.79	1.68	0.45	1.93
HF < 7 yr	0.72	0.57	0.33	0.84	0.82	1.12	0.83	1.64

FIG. 10. Same as in Fig. 9 but for evaporation uncertainty, using E estimated by SLand, ERA-40, and NCEP R2 for the Amazon and NARR for the Mississippi.

surement protocol. We have seen that the diagnosed S is relatively sensitive to persistent imbalance in $P - E$, which contributes to S cumulatively. Should R be "artificially shifted" relative to P from one subperiod to the next, the error would also accumulate together with the real signal. The correction procedure in E^* (section 2a) removes the linear trend (in both signal and error) for the whole period, but the variations are still subject to "subperiod" systematic errors in precipitation and runoff. Such errors are difficult to quantify and will have to be analyzed case by case for individual basins.

7. Comparison with GRACE data

We have shown in section 3 and Fig. 5 that the average Amazon TWS seasonal cycles from GRACE and PER are both about 300 mm. Here we compare the PER results with those of GRACE for the period February 2003–June 2006 (Fig. 11). The resolution of satellite gravity measurement is inherently low, but application is suitable for large basins, such as the Amazon

and Mississippi where the intrinsic error becomes sufficiently small. The data shown in Fig. 11 were produced using a resolution of 500 km, after we also tested other resolutions.

Over the Amazon, the TWS diagnosed from PER method shows overall agreement with the equivalent water thickness from GRACE, such as the small seasonal variation during 2004 and the large increase in 2006. The largest difference occurred at the end of the 2003 dry season when PER method shows 50–100-mm lower water storage. For the Mississippi, the seasonal cycle and much of the interannual variability are similar, but the agreement is somewhat lower than the Amazon. In particular, the PER method shows a general increasing trend from 2004 to 2006 that is not clear in GRACE (but present in the 1000-km resolution data, not shown). Interesting, the interannual variability in the Mississippi is large enough to be comparable to the seasonal cycle, while the Amazon interannual variability is significantly less than its seasonal cycle.

Thus, GRACE data and the PER method show

TABLE 3. Similar to Table 2 but for evaporation using the estimates of SLand, NCEP R2, ERA-40, and NARR.

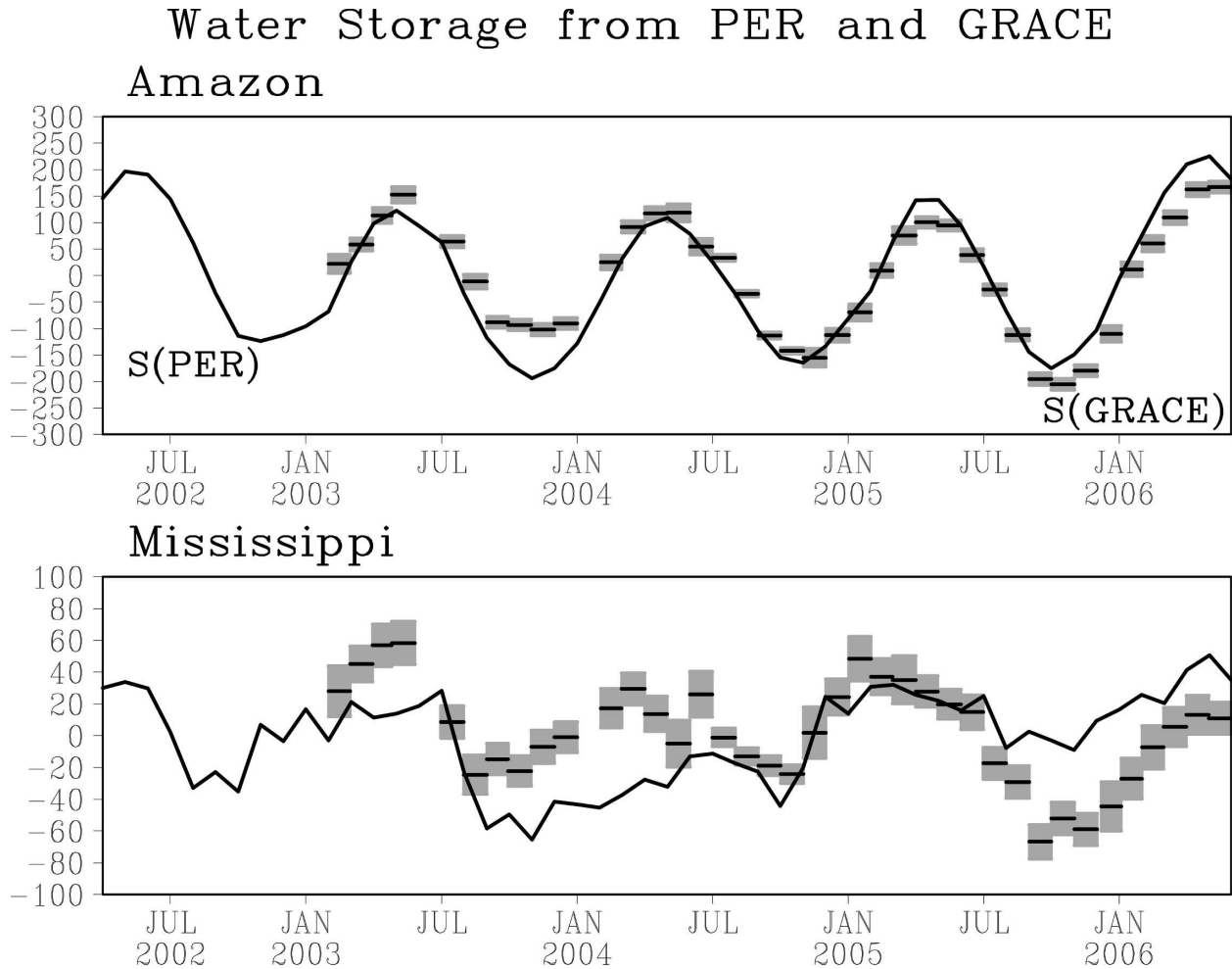|	Amazon				Mississippi			
	NCEP R2/SLand		ERA-40/SLand		NARR/SLand		ERA-40/SLand	
	Corr	σ/σ	Corr	σ/σ	Corr	σ/σ	Corr	σ/σ
Total	0.94	1.47	0.98	1.43	−0.12	0.98	0.69	1.27
HF < 7 yr	0.93	1.15	0.97	1.18	0.29	1.63	0.72	0.84

FIG. 11. Changes in Amazon and Mississippi water storage (mm) from the GRACE satellite gravity measurements (short horizontal bars with shading for error), compared with that from the PER method (solid line).

broadly consistent results for the two basins both for the seasonal cycle and the interannual variability, with the caveat that both methods have their own uncertainties and the overlapping period is too short to statistically verify the water budget approach. It is also interesting to note that while we used estimated evaporation to derive TWS, which is then compared to the GRACE data, recent work has used GRACE TWS as an input to derive evaporation (Rodell et al. 2004b) or $P - E$ (Swenson and Wahr 2006). In both cases, observed P and R are used. These methods essentially look at the same water budget Eq. (2) from a different view angle, and future work is needed to compare such results.

8. Discussion

At first sight, it is surprising that the mere use of observed runoff would lead to much larger S variability in the PER method, compared to a typical offline land model simulation. Both methods use identical P and E, with the only difference that the model simulates its own runoff and the PER method uses observed runoff. This difference is seen clearly by comparing the solid line in Fig. 7b with that in Fig. 7d for the Amazon and Fig. 8b with Fig. 8d for the Mississippi.

Insight comes from a comparison of how R follows P differently in the two cases. Theoretically speaking, because P is the main driving force of land surface hydrology and the water storage "buffering" effect acts as a low-pass filter of the precipitation signal, the subsequent outgoing fluxes, including R (Fig. 3), are damped and delayed responses to P. Indeed, Figs. 12 and 13 show that observed R has an overall interannual amplitude of about 2/3 of P, with a typical lag of about a few months. This damping is larger on a seasonal time scale (Fig. 6a). Such a relationship can be shown easily
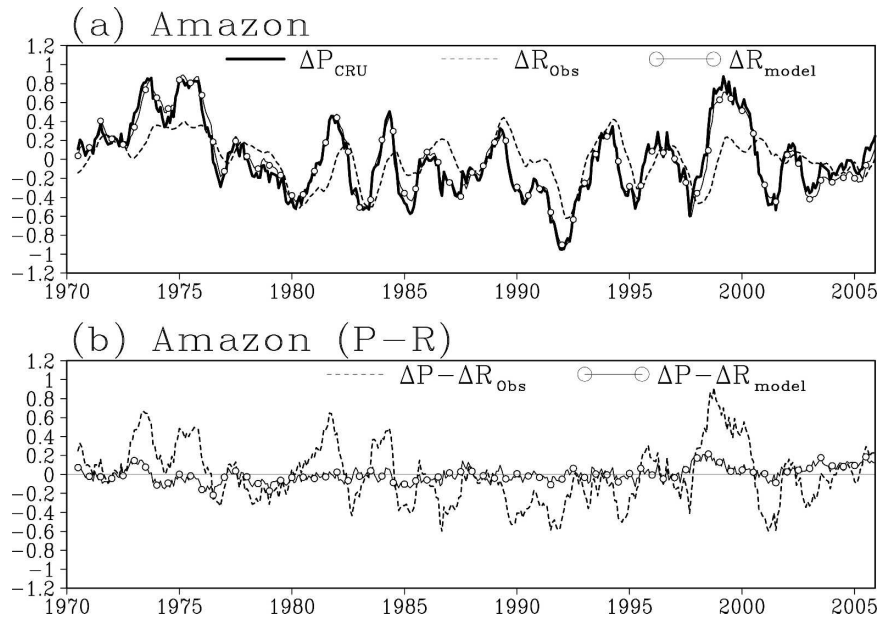
FIG. 12. (a) Anomalies of observed and modeled (SLand) runoff against precipitation (mm day^{-1}); (b) differences between observed precipitation and observed (dashed) and modeled (line with open circles) runoff. The observed runoff is more different from observed precipitation especially over the Amazon, implying the large capacity of land to store water that is underrepresented by models.

with mathematical rigor in simple first-order force-damped equations, such as Eq. (2) in the special case of a single intrinsic time scale. The most important point here is that the modeled R follows P much too closely compared to observed R, both in terms of amplitude and phasing. As a result, modeled R has a stronger tendency to cancel out changes in precipitation so that the difference $P - E$ is much smaller than observed
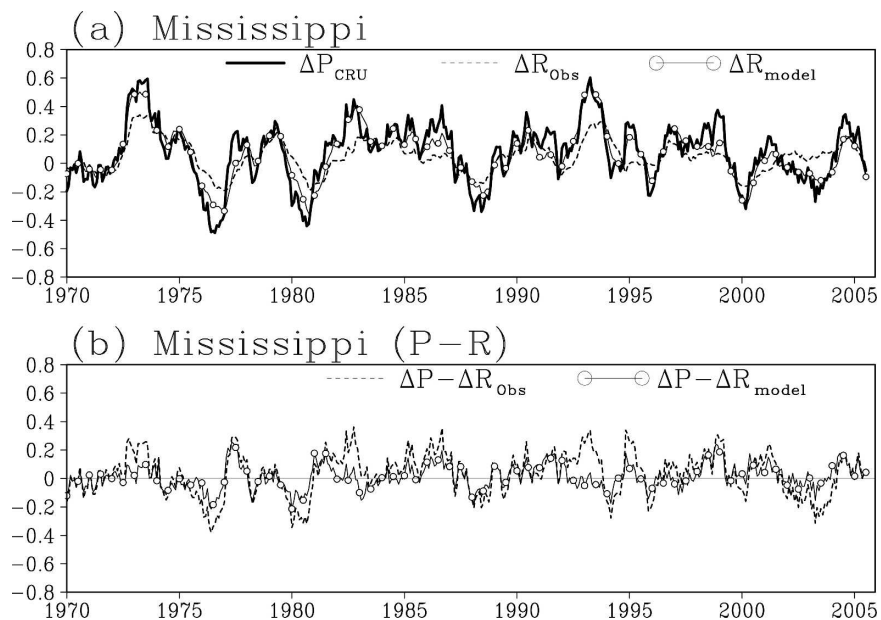

FIG. 13. Same as in Fig. 12 but for the Mississippi basin. The modeled R captures more of the observed variability than for the Amazon.

(Figs. 12, 13), thus leading to smaller variability in the diagnosed S (neglecting E variability; section 2b). This is especially the case for the Amazon and explains why the models severely underestimate TWS variability there (section 4 and Fig. 7d). For the Mississippi, the model-simulated amplitude in S (Fig. 8d) is closer to that diagnosed (Fig. 8c) on the interannual time scale (though still largely underestimated on decadal and longer time scales), consistent with the fact that the model $P - E$ is much closer to observed (Fig. 13). It is probably not surprising that the model does a poorer job over the Amazon than the Mississippi because the Amazon rain forest likely has larger dynamic range due to the deep soil and deep roots.

Such a damped and significantly delayed response of runoff to precipitation suggests the large capacity of land surface in storing and taking up water, a capacity models appear to significantly underrepresent. To put it another way, real land surface seems to be able to hold up more water from wet episodes, and then uses it more slowly during dry periods, while models tend to have overly sensitive runoff response that flushes out "excessive" water too quickly.

9. Conclusions

Applying the basin water budget equation in the PER method for the Amazon and the Mississippi basins, we found changes of 100–200 mm on interannual time scales and 600–800 mm over multidecadal time scales in terrestrial total water storage for these two basins. Such large change especially on longer time scales is remarkable, as many land surface models have field capacity (the maximum change in soil moisture a model can produce) comparable or smaller than this.

Theoretically speaking, the diagnosed TWS variability is larger than or equal to any modeled soil moisture variability because the diagnosis includes all the possible changes in the basin, including surface and underground water and water stored in vegetation, while models typically only simulate soil moisture change in the top 1–2 m. For example, during flooding season, the Amazon River expands into adjacent forest and the surface water can account for up to 10% of the seasonal soil moisture change. However, the major contributor missing in simple land surface models is likely the deeper soil moisture storage and groundwater. Such deep water storage is utilized by deep roots. In one instance, Nepstad et al. (1994) found deep root water uptake down to 8 m below the surface that sustained normal growth during a prolonged dry period. Even deeper roots have been observed in many other regions (Schenk and Jackson 2005). More sophisticated models

may include several soil layers, which would increase the effective filed capacity and thus the amplitude of variation. However, the lack of deep roots may prevent the model to utilize deep water storage as efficiently as nature does. Our analysis with a simple model suggests that model runoff may respond too quickly to remove excessive precipitation such that soil moisture variability is small, regardless of the specified field capacity. It is worth noting that even if a model simulates a good mean seasonal cycle in runoff [as is often validated in a model intercomparison project, such as the Global Soil Wetness Project (GSWP)], it does not guarantee a good simulation of interannual variability, as it is the difference in P and R that matters most to water storage (section 6 above). Projects, such as GSWP-2 (http://www.iges.org/gswp2/), are expected to make available longer-term simulations where interannual variability can be assessed. Because of the sensitivity of cumulative TWS to the imbalance between P, E, and R [Eq. (3) and section 6], any persistent error will accumulate and manifest itself in the integrated TWS as long-term change. Thus the PER method can easily overestimate long-term TWS changes for small but persistent systematic error in P, E, and R. The simple error analysis (section 6) suggests an uncertainty of factor of 2 on decadal and longer time scales. Despite such a caveat, the large changes on decadal to multidecadal time scales found here suggest that current models may significantly underestimate such variations. An important implication is that land surface may have a memory beyond 1-yr related to the change in the total water storage,[1] significantly longer than the typically cited 1 month to 1 season.

The PER basin budget method uses observed precipitation and runoff, combined with estimated evapotranspiration, to estimate the change in total land water storage. The land water budget equation [Eq. (2)] is simple and has been used for various purposes (e.g., Mintz and Walker 1993). But to our knowledge, it had not been applied for long-term water storage variability in a way similar to the PER method discussed here. Our preliminary analysis suggests its ability in depicting long-term water storage change, in a way significantly more robust than the moisture convergence method. The results will thus provide an important means to cross-validate other methods, such as GRACE data. If such comparison leads to confidence in both methods over the period when satellite is available (recent years

---

[1] In a simplistic way, time scale can be estimated as capacity divided by flux. Assuming a field capacity of 1000 mm for the Amazon, then the time scale is 1000 mm/(5 mm day^{-1}) = 200 days.

and near future) as suggested by this work, they will provide important information on water storage variability in major periods of the twentieth century when the basin budget method is applicable. They can also provide validated approaches for long-term land water monitoring in the future.

REFERENCES

Amenu, G. G., P. Kumar, and X.-Z. Liang, 2005: Interannual variability of deep-layer hydrologic memory and mechanisms of its influence on surface energy fluxes. *J. Climate,* **18,** 5024–5045.

Betts, A. K., J. H. Ball, P. Viterbo, A. Dai, and J. Marengo, 2005: Hydrometeorology of the Amazon in ERA-40. *J. Hydrometeor.,* **6,** 764–774.

Chen, M., P. Xie, J. E. Janowiak, and P. A. Arkin, 2002: Global land precipitation: A 50-yr monthly analysis based on gauge observations. *J. Hydrometeor.,* **3,** 249–266.

Dai, Y., and Coauthors, 2003: The Common Land Model. *Bull. Amer. Meteor. Soc.,* **84,** 1013–1023.

Davis, E. A., and C. P. Pase, 1977: Root systems of shrub live oak: Implications for water yield in Arizona chaparral. *J. Soil Water Conserv.,* **32,** 174–180.

Delworth, T. L., and S. Manabe, 1993: Climate variability and land-surface processes. *Adv. Water Res.,* **16,** 3–20.

Dirmeyer, P. A., A. J. Dolman, and N. Sato, 1999: The pilot phase of the Global Soil Wetness Project. *Bull. Amer. Meteor. Soc.,* **80,** 851–878.

Engman, E. T., and N. Chauhan, 1995: Status of microwave soil moisture measurements with remote sensing. *Remote Sens. Environ.,* **51,** 189–198.

Fan, Y., and H. Van den Dool, 2004: Climate Prediction Center global monthly soil moisture data set at 0.5 degrees resolution for 1948 to present. *J. Geophys. Res.,* **109,** D10102, doi:10.1029/2003JD004345.

Gibson, J. K., P. Kållberg, S. Uppala, A. Hernandez, A. Nomura, and E. Serrano, 1997: ERA description. ECMWF Reanalysis Project Report Series 1, Shinfield Park, Reading, United Kingdom, 72 pp.

Hansen, J., R. Ruedy, J. Glascoe, and M. Sato, 1999: GISS analysis of surface temperature change. *J. Geophys. Res.,* **104,** 30 997–31 022.

Hoerling, M., and A. Kumar, 2003: The perfect ocean for drought. *Science,* **299,** 691–694.

Hollinger, S. E., and S. A. Isard, 1994: A soil moisture climatology of Illinois. *J. Climate,* **7,** 822–833.

Jackson, R. B., L. A. Moore, W. A. Hoffmann, W. T. Pockman, and C. R. Linder, 1999: Ecosystem rooting depth determined with caves and DNA. *Proc. Natl. Acad. Sci. USA,* **96,** 11 387–11 392.

——, and Coauthors, 2000: Belowground consequences of vegetation change and their treatment in models. *Ecol. Appl.,* **10,** 470–483.

Kalnay, E., and Coauthors, 1996: The NCEP/NCAR 40-Year Reanalysis Project. *Bull. Amer. Meteor. Soc.,* **77,** 437–471.

Kanamitsu, M., W. Ebisuzaki, J. Woollen, S.-K. Yang, J. J. Hnilo, M. Fiorino, and G. L. Potter, 2002: NCEP–DOE AMIP-II Reanalysis (R-2). *Bull. Amer. Meteor. Soc.,* **83,** 1631–1643.

Kleidon, A., and M. Heimann, 2000: Assessing the role of deep rooted vegetation in the climate system with model simulations: Mechanism, comparison to observations and implications for Amazonian deforestation. *Climate Dyn.,* **16,** 183–199.

Koster, R. D., and Coauthors, 2004: Regions of strong coupling between soil moisture and precipitation. *Science,* **305,** 1138–1140.

Manabe, S., J. Smagorinsky, and R. F. Strickler, 1965: Simulated climatology of a general circulation model with a hydrologic cycle. *Mon. Wea. Rev.,* **93,** 769–798.

Masuda, K., Y. Hashimoto, H. Matsuyama, and T. Oki, 2001: Seasonal cycle of water storage in major river basins of the world. *Geophys. Res. Lett.,* **28,** 3215–3218.

Mesinger, F., and Coauthors, 2006: North American regional reanalysis. *Bull. Amer. Meteor. Soc.,* **87,** 343–360.

Mintz, Y., and G. K. Walker, 1993: Global fields of soil moisture and land surface evapotranspiration derived from observed precipitation and surface air temperature. *J. Appl. Meteor.,* **32,** 1305–1334.

Mitchell, T. D., and P. D. Jones, 2005: An improved method of constructing a database of monthly climate observations and associated high-resolution grids. *Int. J. Climatol.,* **25,** 693–712.

Nepstad, D. C., and Coauthors, 1994: The role of deep roots in the hydrological and carbon cycles of Amazonian forests and pastures. *Nature,* **372,** 666–669.

New, M., M. Hulme, and P. Jones, 1999: Representing twentieth-century space–time climate variability. Part I: Development of a 1961–90 mean monthly terrestrial climatology. *J. Climate,* **12,** 829–856.

Qian, T., A. Dai, and K. E. Trenberth, 2007: Hydroclimatic trends in the Mississippi River basin from 1948 to 2004. *J. Climate,* **20,** 4599–4614.

Rasmusson, E. M., 1968: Atmospheric water vapor transport and the water balance of North America. II: Large-scale water balance investigations. *Mon. Wea. Rev.,* **96,** 720–734.

Roads, J. O., S.-C. Chen, A. K. Guetter, and K. P. Georgakakos, 1994: Large-scale aspects of the United States hydrologic cycle. *Bull. Amer. Meteor. Soc.,* **75,** 1589–1610.

Robock, A., K. Y. Vinnikov, G. Srinivasan, J. K. Entin, S. E. Hollinger, N. A. Speranskaya, S. Liu, and A. Namkhai, 2000: The Global Soil Moisture Data Bank. *Bull. Amer. Meteor. Soc.,* **81,** 1281–1299.

——, M. Mu, K. Vinnikov, I. V. Trofimova, and T. I. Adamenko, 2005: Forty-five years of observed soil moisture in the Ukraine: No summer desiccation (yet). *Geophys. Res. Lett.,* **32,** L03401, doi:10.1029/2004GL021914.

Rodell, M., and J. S. Famiglietti, 2001: An analysis of terrestrial water storage variations in Illinois with implications for the Gravity Recovery and Climate Experiment (GRACE). *Water Resour. Res.,* **37,** 1327–1340.

——, and Coauthors, 2004a: The global land data assimilation system. *Bull. Amer. Meteor. Soc.,* **85,** 381–394.

——, J. S. Famiglietti, J. Chen, S. Seneviratne, P. Viterbo, S. Holl, and C. R. Wilson, 2004b: Basin scale estimates of evapotranspiration using GRACE and other observations. *Geophys. Res. Lett.,* **31,** L20504, doi:10.1029/2004GL020873.

Schenk, H. J., and R. B. Jackson, 2005: Mapping the global distribution of deep roots in relation to climate and soil characteristics. *Geoderma,* **126,** 129–140.

Schubert, S. D., R. B. Rood, and J. Pfaendtner, 1993: An assimilated dataset for earth science applications. *Bull. Amer. Meteor. Soc.,* **74,** 2331–2342.

Seager, R., Y. Kushnir, C. Herweijer, N. Naik, and J. Velez, 2005: Modeling of tropical forcing of persistent droughts and pluvials over western North America: 1856–2000. *J. Climate,* **18,** 4065–4088.

Seneviratne, S. I., P. Viterbo, D. Lüthi, and C. Schär, 2004: Inferring changes in terrestrial water storage using ERA-40 reanalysis data: The Mississippi River basin. *J. Climate,* **17,** 2039–2057.

Shao, Y., and A. Henderson-Sellers, 1996: Modeling soil moisture: A project for intercomparison of land surface parameterization schemes phase 2(b). *J. Geophys. Res.,* **101,** 7227–7250.

Shuttleworth, W. J., 1988: Evaporation from Amazonian rainforest. *Proc. Roy. Soc. London,* **233,** 321–346.

Swenson, S., and J. Wahr, 2006: Estimating large-scale precipitation minus evapotranspiration from GRACE satellite gravity measurements. *J. Hydrometeor.,* **7,** 252–270.

Tapley, B. D., S. Bettadpur, M. Watkins, and C. Reigber, 2004: The gravity recovery and climate experiment: Mission overview and early results. *Geophys. Res. Lett.,* **31,** L09607, doi:10.1029/2004GL019920.

Wahr, J., S. Swenson, V. Zlotnicki, and I. Velicogna, 2004: Time-variable gravity from GRACE: First results. *Geophys. Res. Lett.,* **31,** L11501, doi:10.1029/2004GL019779.

Werth, D., and R. Avissar, 2004: The regional evapotranspiration of the Amazon. *J. Hydrometeor.,* **5,** 100–109.

Xie, P., and P. A. Arkin, 1996: Analyses of global monthly precipitation using gauge observations, satellite estimates, and numerical model predictions. *J. Climate,* **9,** 840–858.

Yeh, P. J.-F., M. Irizarry, and E. A. B. Eltahir, 1998: Hydroclimatology of Illinois: A comparison of monthly evaporation estimates based on atmospheric water balance and soil water balance. *J. Geophys. Res.,* **103,** 19 823–19 838.

Yeh, T.-C., R. T. Wetherald, and S. Manabe, 1984: The effect of soil moisture on the short-term climate and hydrology change—A numerical experiment. *Mon. Wea. Rev.,* **112,** 474–490.

Zeng, N., 1999: Seasonal cycle and interannual variability in the Amazon hydrologic cycle. *J. Geophys. Res.,* **104,** 9097–9106.

——, J. D. Neelin, K.-M. Lau, and C. J. Tucker, 1999: Enhancement of interdecadal climate variability in the Sahel by vegetation interaction. *Science,* **286,** 1537–1540.

——, ——, and C. Chou, 2000: A quasi-equilibrium tropical circulation model—Implementation and simulation. *J. Atmos. Sci.,* **57,** 1767–1796.

——, A. Mariotti, and P. Wetzel, 2005: Terrestrial mechanisms of interannual CO_2 variability. *Global Biogeochem. Cycles,* **19,** GB1016, doi:10.1029/2004GB002273.